High Temperature Strengthening Mechanisms in the Alloy Platinum-5% Rhodium DPH

Investigation of dispersion strengthened platinum alloy for high temperature applications

http://dx.doi.org/10.1595/147106711X591971 http://www.platinummetalsreview.com/

By Katharina Teichmann, Christian H. Liebscher and Rainer Völkl*

Metals and Alloys, University Bayreuth, Ludwig-Thoma-Straße 36b, D-95447 Bayreuth, Germany

*Email: rainer.voelkl@uni-bayreuth.de

Stefan Vorberg

W. C. Heraeus GmbH, Heraeusstraße 12–14, D-63450 Hanau, Germany

Uwe Glatzel

Metals and Alloys, University Bayreuth, Ludwig-Thoma-Straße 36b, D-95447 Bayreuth, Germany

To improve the high temperature properties, platinum can be hardened by solid solution and/or oxide particles. The investigated alloy, dispersion hardened platinum-5% rhodium (Pt-5%Rh DPH), was produced via melting and subsequent annealing of the semi-finished product in order to obtain an oxide particle dispersion. Despite the relatively large oxide particles formed in this process, the creep strength is much higher in comparison to conventional Pt-5%Rh. The aim of this paper is to study the strengthening mechanisms in the alloy Pt-5%Rh DPH by transmission and scanning electron microscopy. The size distribution of oxide particles shows a bimodal distribution, and the average oxide particle diameter is 315 nm for particles larger than 150 nm. For particles between 25 nm and 150 nm the average diameter is 49 nm. The size ranges of oxide particles are not substantially affected by high temperature creep deformation, but particles of <25 nm evolve during high temperature creep. It was found that all particles of different size ranges interact with dislocations and hence contribute to the strengthening of Pt-5%Rh DPH. Dislocation forests are pinned on the surface of oxide particles larger than 150 nm in diameter. Dislocation pile ups form between particles with a size range of about 500 nm. Medium size and small particles of diameters between 50 nm and 10 nm act as obstacles to single dislocations through backside pinning.

Introduction

Platinum-rhodium alloys can be used under high chemical, mechanical and thermal loadings due to the high melting point of platinum (1770ºC), and its exceptional corrosion and oxidation resistance up to high temperatures. The creep strength of platinum materials is improved by solid solution hardening and/or by oxide dispersions (1). For strengthening by solid solution the elements rhodium and iridium

are added. Besides the hardening effect, the melting point is also raised. A fine dispersion of oxide particles in the metallic matrix may also improve creep strength (2–5).

Most platinum fabricators offer oxide dispersion strengthened platinum alloys (ODS alloys). The production of ODS alloys is based on various principles. Several authors (4, 6) describe the mechanical alloying of platinum powder with zirconia and/or yttria powders. A wet chemical coprecipitation of a platinum and zirconyl chloride powder can also produce a fine metal ceramic powder mixture (7). In both cases a subsequent powder metallurgical processing results in semi-finished products.

An alternative preparation route to disperse fine oxide particles is the internal oxidation of a platinum alloy containing elements with a high oxygen affinity (8). However, the complete internal oxidation of semi-finished platinum products was long considered to be unlikely because of the limited solubility and diffusivity of oxygen in platinum. Hence, the internal oxidation of semi-finished platinum products would require very long times for the heat treatment which would involve strong grain growth in the inner and not yet oxidised material as well as oxide formation at the grain boundaries. Both effects are considered to cause brittleness. To overcome these difficulties the volume of the oxidised material is reduced, and measures to accelerate the internal oxidation are taken. A possible manufacturing route is the internal oxidation of powder or turnings of Pt-Zr alloys in air and again a subsequent powder metallurgical processing to semi-finished products (9). Fine liquid drops of a platinum alloy with reactive constituents may already be internally oxidised during a spray process of the molten alloy in a cold mould in an oxidising atmosphere (10). The ingot is then worked down to products like wires or sheets. Thin foils of a Pt-Zr alloy can be internally oxidised reasonably quickly at higher temperatures in air. A stack of these thin internally oxidised foils can subsequently be welded together to form sheet material by hot rolling (11).

W. C. Heraeus GmbH developed a family of ODS platinum materials called DPH. In a first production step zirconium, yttrium and cerium are added to a platinum melt in elemental form and the molten alloy is cast to ingots. During a subsequent operation semi-finished products, like sheets, tubes and rods, are annealed in an oxidising atmosphere leading to the internal oxidation of the bulk platinum alloy. The internal oxidation leads to the formation of finely dispersed oxide particles of the elements with high affinity for oxygen, i.e. Zr, Y and Ce (12, 13). The fundamental differences to the internal oxidation processes described above are that large volumes of semi-finished platinum parts are internally oxidised in short times and no powder metallurgical processes are involved.

These DPH materials overcome the disadvantages of previously known ODS materials produced by powder metallurgy, for example the difficulties in fabrication, especially in welding, and their limited ductility (14). Furthermore these materials show a great improvement of the creep properties in comparison to the solid solution hardened Pt-Rh and Pt-Ir alloys (14). This is remarkable, since the mean particle size, as known so far, is bigger than that obtained *via* the powder metallurgical route and exceeds the value for optimal strengthening given by Bürgel (15). The mechanism of strengthening by oxide particle dispersion is the interaction between particles and dislocations as discussed in the present paper (1, 16–20). The Pt-5%Rh DPH alloy was developed as an alternative material to the widely used Pt-10%Rh DPH alloy mainly for applications in the glass industry as fibre bushings, plungers and stirrers with reduced Rh content, due to the steadily increasing Rh price (21).

In this work we focus on the investigation of creep deformed Pt-5%Rh DPH sheets using scanning electron microscopy (SEM) and transmission electron microscopy (TEM) to study the strengthening mechanisms.

Experimental

The material investigated was Pt-5%Rh DPH produced by Heraeus and containing up to 1 wt% Zr, Y and Ce (13). The creep specimens were wire cut from a 0.87 mm thick sheet which had undergone a standard thermomechanical finishing process. Creep tests were carried out at 1600ºC under a load of 5 MPa in air using a tensile creep test device developed in-house (22–24). To analyse the microstructure and especially the evolution of the dislocation structure, the creep tests were interrupted after different time periods. TEM samples were prepared from the crept specimens by mechanically grinding and successive electrochemical twin-jet polishing with a dilute aqueous potassium cyanide solution at 18ºC and 30 V until a hole appeared in the sample.

All SEM images were acquired using a ZEISS 1540EsB CrossBeam® workstation. The particle size distribution was determined from SEM images of the ground and polished TEM samples, where at least ten images with an average number of 170 particles per image were measured. The area fraction method was used.

All TEM investigations were carried out with a ZEISS Libra 200 FE equipped with an OMEGA energy filter. Measurements using energy filtered transmission electron microscopy (EFTEM) (25) were performed to investigate the local distribution of elements. This method is based on electron energy loss spectroscopy (EELS) in combination with imaging in the TEM using inelastic processes of inner-shell electron excitations. The advantage of EELS and EFTEM measurements is the high spatial resolution of below 1 nm and high energy resolution of about 1 eV (26,27).

Results

Tensile Creep Testing

The first specimen ruptured after 17 h creep at 1600°C under a load of 5 MPa in air (**Figure 1**). On the basis of this creep curve, it was decided to perform additional creep tests and interrupt these (fast cool down under load) after 1 h and 8 h respectively in order to investigate the change in the microstructure.

The observed decrease in strain after about 1 h during the 1 h and 17 h creep tests was thought to be due to poor temperature control. A change in the specimen surface caused a variation of its emissivity. Because a pyrometer was used, the actual temperature of the specimen was therefore higher than measured in the early creep stage, leading to thermal strains which add to the creep strains shown in **Figure 1**. The temperature control of the sample interrupted after 8 h creep deformation was more accurate, so that no thermal strains were added during the first creep stage. Specimens of the ruptured sample and the sample interrupted after 8 h high temperature creep were used for TEM analysis.

SEM Investigations of the Oxide Particle Distribution

The oxide particle distribution is important for the high temperature strength properties (16). This includes both the location and size distribution of the oxide particles. Due to the thermomechanical finishing process the microstructure consists of elongated, aligned grains with an average grain aspect ratio of 5 (**Figure 2(a)**). In **Figure 2(b)** the local distribution of the oxide particles is shown. Large oxide particles are primarily situated at the grain boundaries, whereas finely dispersed particles can be found inside the

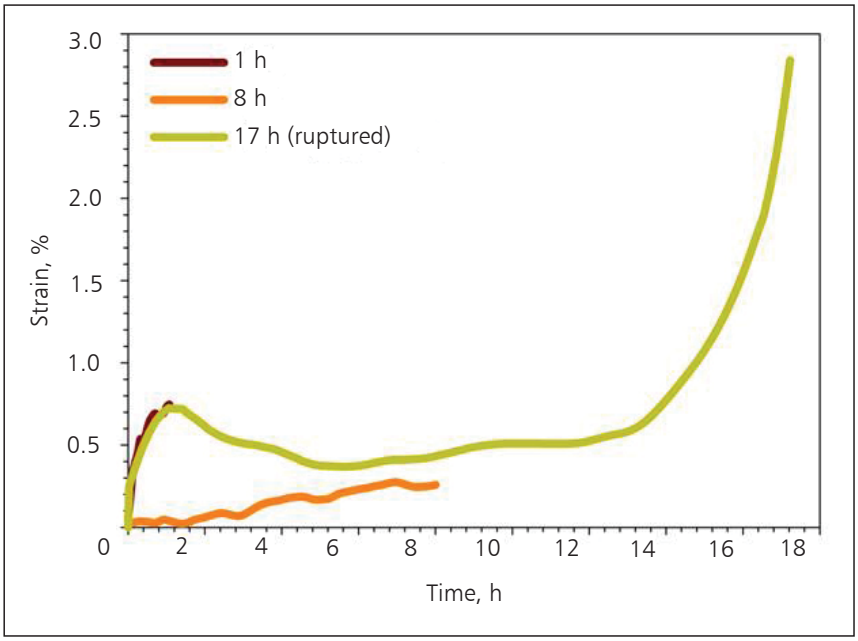

Fig. 1. Creep curves of Pt-5%Rh DPH tested at T = 1600°C under a load of σ = 5 MPa in air

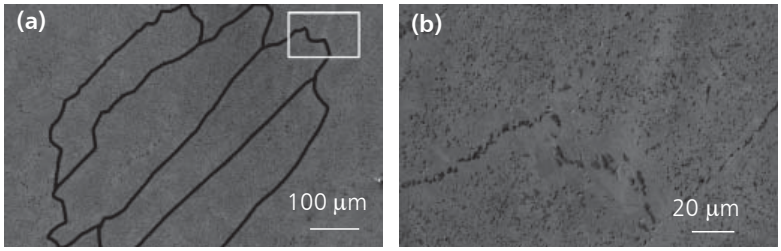

Fig. 2(a). Microstructure of the Pt-5%Rh DPH alloy after thermomechanical treatment; (b) location distribution of the oxide particles inside the grains and on the grain boundaries of the area indicated by the white rectangle of Figure 2(a)

grains. This can be traced back to the production route of internal oxidation, as the oxygen solubility and the nucleation rate is higher at the grain boundaries than inside the grains (28).

Figure 3 shows the size distribution of particles (particle count) inside the grains for Pt-5%Rh DPH in the as received condition. The oxide particles inside the grains show a bimodal size distribution. The maximum of 60% for the particles smaller than 150 nm falls in the range between 25–50 nm with an average diameter of 49 ± 22 nm. Particles with diameters smaller than 25 nm can hardly be resolved in the SEM and are therefore neglected in the description of the particle size distribution. For particles larger than 150 nm, 65% have diameters between 150–300 nm and the average diameter is 315 ± 34 nm. The average particle diameter increases to 342 ± 26 nm for the ruptured sample after 17 h creep deformation, but is within the scatter of the measurements. The initial average size of oxide particles is therefore smaller than for the Pt DPH alloy reported by Vorberg *et al.* (29). Particles with diameters smaller than 25 nm could not be found either on SEM or on TEM micrographs of Pt-5%Rh DPH in the as received condition. However, particles with diameters of <25 nm are present in the ruptured sample and contribute to the strengthening of the Pt-5%Rh DPH alloy, as shown in the following section.

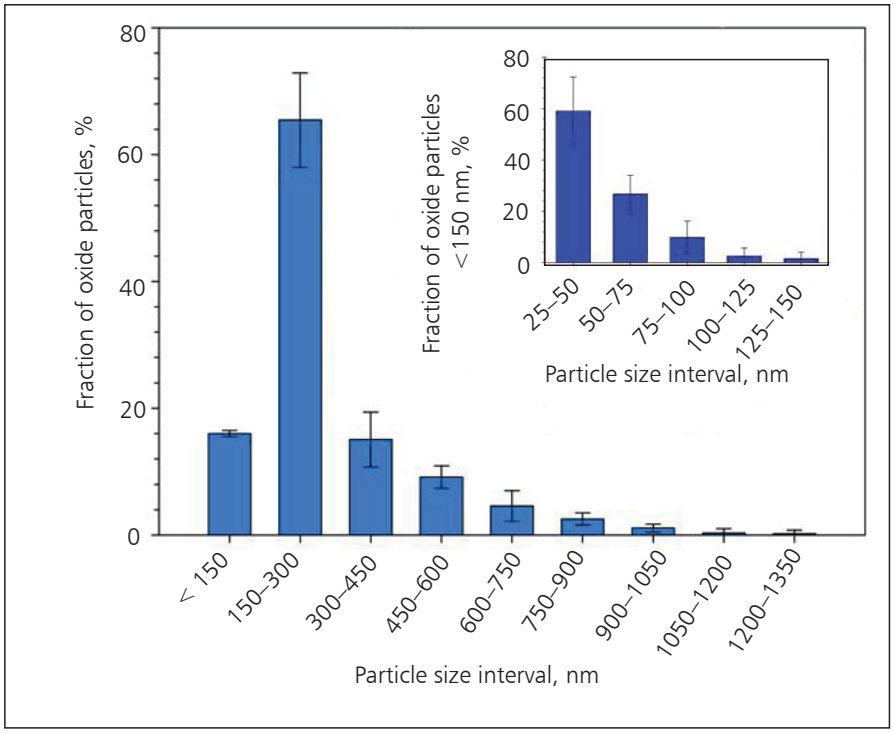

Fig. 3. Size distribution of oxide particles in Pt-5%Rh DPH as received; the small insert shows the size distribution of oxide particles from 25 to 150 nm

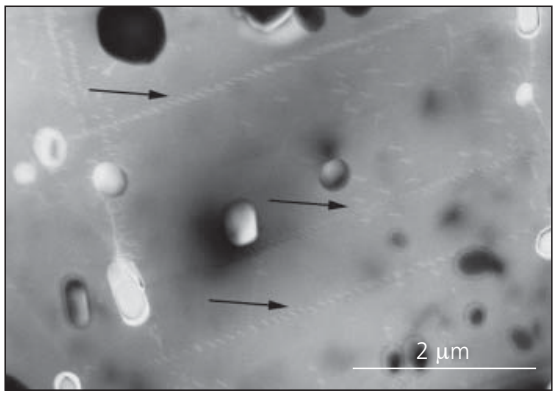

Fig. 4. Scanning TEM image of low angle boundaries of the Pt-5%Rh DPH sample interrupted after 8 h creep deformation

TEM Investigations of Particle–Dislocation Interactions

After 8 h of creep deformation at 1600ºC dislocation pile-ups are observed on oxide particles with diameters above about 500 nm in the Pt-5%Rh DPH sample (**Figure 4**). The Burgers vector was determined using the $\vec{g} \times \vec{b} = 0$ criterion ($\vec{g}$ = diffraction vector, $\vec{b}$ = Burgers vector) (30). Under two different two-beam conditions the Burgers vector in the pile-up was determined to be $\pm a/2[01\bar{1}]$ (a = lattice parameter). All dislocations in a pile-up have the same Burgers vector, hence forming a low angle grain boundary.

Small particles are invisible under the two-beam bright-field (BF) condition, but can be resolved under weak-beam dark-field (WBDF) conditions (**Figure 5**). The reason is that under weak-beam conditions the thickness of dislocation lines is smaller and the contrast is higher, because only the part of a dislocation with the biggest strain field (the dislocation core) contributes to the contrast (31, 32). Thus the weak-beam method is a useful tool to investigate the interaction mechanisms between dislocations and particles (33).

Strong bowing of dislocations around oxide particles with diameters of less than 50 nm is observed in Pt-5%Rh DPH after 8 h high-temperature creep, indicating a pinning of dislocations at the incoherent interface between matrix and particles (positions A in **Figure 6**). Dislocations obviously do not shear these incoherent, medium sized particles but climb over them (**Figure 7(a)**), followed by backside pinning at the interface between matrix and particle (**Figure 7(b)**). According to Arzt and Rösler (34, 35), the detachment of the dislocation from the particle is the decisive step slowing down dislocation movement, hence increasing creep strength. Bypassing of the particles by the Orowan mechanism (15) is not seen.

The pinning of a dislocation on the backside of an oxide particle with a diameter of less than 10 nm immediately before being detached is clearly resolved in the WBDF image of **Figure 6** at position B. This indicates that the dislocation is immobilised by an attractive force after completing the climb process over the particle. Additional energy is therefore required to detach the dislocation from the matrix/particle interface, contributing to the creep strength of Pt-5%Rh DPH (35). A particle of less than 10 nm in diameter, not connected with a dislocation, can be seen at position C in **Figures 6(a)** and **6(b)**. To prove that the bright areas in WBDF images and the corresponding dark areas in BF images with diameters in the range of 10–25 nm are particles, EFTEM measurements were carried out. The EEL spectra of **Figure 8(b)** were extracted from an series of 21 energy filtered images acquired in an energy loss window from 127–207 eV. The EEL spectrum extracted from point 1 in **Figure 8(a)** clearly shows the Y-M_{45} and Zr-M_{45} edges proving the presence of an

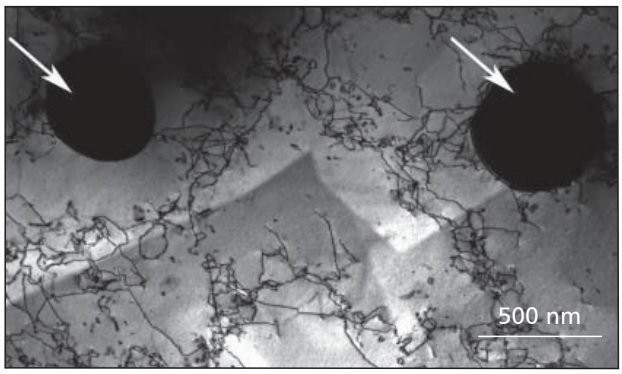

Fig. 5. Two oxide particles surrounded by dislocation forests in the ruptured Pt-5%Rh DPH sample

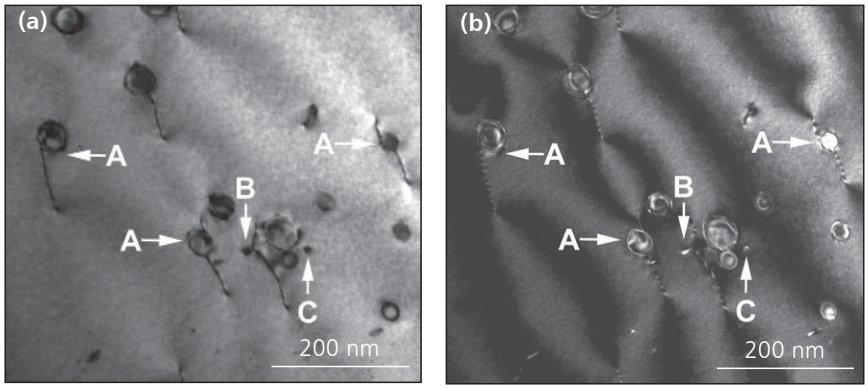

Fig. 6(a). Bright-field TEM image of dislocation–particle interaction mechanisms in Pt-5%Rh DPH after 8 h creep at 1600°C; (b) corresponding weak-beam dark-field image

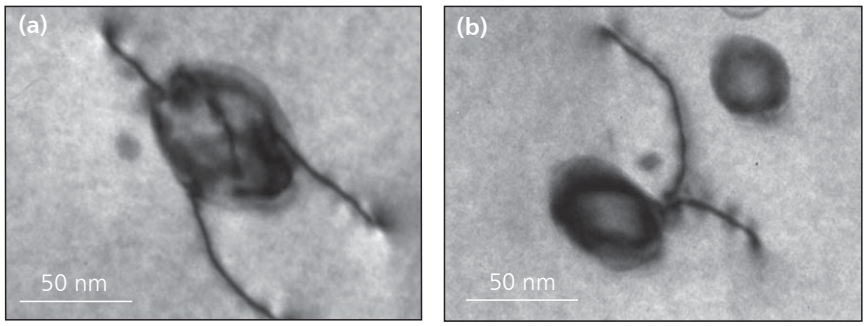

Fig. 7(a). Climbing of dislocations over an oxide particle; (b) backside pinning of a dislocation in the matrix/particle interface

Y and Zr containing particle, most likely a Zr/Y mixed oxide. To exclude effects from dislocation contrast on the acquired energy filtered images, a second spectrum was extracted from point 2 in **Figure 8(a)**. The corresponding EEL spectrum in **Figure 8(b)** shows no absorption edges.

The observed interaction mechanisms of dislocations with oxide particles are in agreement with observations made by Häussler *et al.* (18) and Bartsch *et al.* (36) for ODS nickel-base superalloys. Also a comparison with the ODS NiAl alloy investigated by Behr *et al.* (20) and the alloy Inconel MA 754

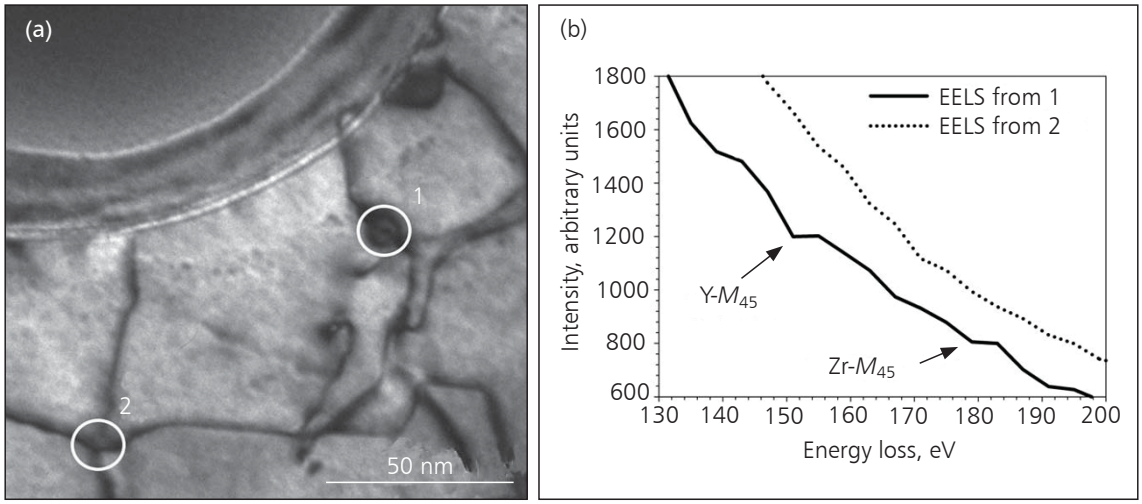

Fig. 8(a). Zero loss bright-field TEM image of the analysed area for EFTEM measurements in Pt-5%Rh DPH after 17 h creep until rupture at 1600°C; (b) extracted EEL spectra of areas 1 and 2 of Figure 8(a)

investigated by Nardone *et al.* (37) confirm the strengthening mechanisms observed in the examined Pt-5%Rh DPH alloy.

Conclusions

The Pt-5%Rh DPH alloy shows an elongated grain structure after the thermomechanical finishing process. Scanning electron microscopy reveals oxide particles of diameters larger than 1 μm at grain boundaries. In the as received condition a bimodal particle size distribution is found inside the grains. The average particle diameter of the initial state is 315 nm and remains almost unchanged after high temperature creep deformation for 17 h. This observation is in contrast to measurements carried out by Vorberg *et al.* (29) in Pt DPH, where the average particle diameter increases from 400 nm to 550 nm after 10 h creep deformation at 1600ºC. Particles with diameters of less than 25 nm could not be found in the alloy as received. However, imaging and electron spectroscopy analysis clearly demonstrates that oxide particles of less than 25 nm in diameter are present in the alloy after 8 h and 17 h creep at 1600ºC. Hence this very fine fraction of oxide particles evolves during creep and interacts with dislocations, hindering their movement through backside pinning.

Various mechanisms slowing down creep deformation of Pt-5%Rh DPH at 1600ºC have been confirmed. It has been shown that dislocations interact with oxide particles of all sizes as follows:

- Dislocation pile-ups forming low angle grain boundaries are found at oxide particles with diameters above about 500 nm.
- Dislocations organised in forests are pinned at the surfaces of oxide particles in the range of 150–500 nm.
- Medium sized oxide particles around 50 nm force non-conservative dislocation climb followed by backside pinning.
- Kinked dislocations indicate that very small particles below 25 nm also pin dislocations.

The observed dislocation interactions with oxide particles of all size ranges are in general agreement with observations in Pt DPH (29). However, the stress to rupture of the Pt-5%Rh DPH alloy during creep testing at 1600ºC is higher than values measured for Pt-10%Rh, Pt DPH and Pt-5%Au DPH (38). In comparison to Pt DPH, the higher creep strength is believed to originate from a larger fraction of oxide particles with diameters of less than 150 nm in Pt-5%Rh DPH than found in Pt DPH (29). In general, the observed strengthening mechanisms by the oxide particles of different size ranges lead to the deceleration of creep deformation of Pt-5%Rh DPH at 1600ºC compared to pure Pt and solid solution strengthened Pt-5%Rh and Pt-10%Rh.

References

1 B. Reppich, F. Brungs, G. Hümmer and H. Schmidt, 'Modelling of the Creep Behaviour of ODS Platinum-Based Alloys', in "Proceedings of the Fourth International Conference on Creep and Fracture of Engineering Materials and Structures", eds. B. Wilshire and R. W. Evans, The Institute of Metals, London, UK, 1990, pp. 142–158

2 D. F. Lupton, *Adv. Mater.*, 1990, (5), 29

3 M. V. Whalen, *Platinum Metals Rev.*, 1988, **32**, (1), 2

4 H. A. Jansen and F. A. Thompson, *Glastech. Ber.*, 1992, **65**, (4), 99

5 J. Stokes, *Platinum Metals Rev.*, 1987, **31**, (2), 54

6 F. K. Roehrig, Owens-Corning Fiberglass Corp, 'Process for Producing Dispersion Strengthened Precious Metal Alloys', *World Appl.* 81/00,977

7 G. Hammer, D. Kaufmann and M. Clasing, *Metall*, 1981, **35**, (7), 531

8 G. Reinacher, *Z. Metallkd.*, 1971, **62**, (11), 835

9 G. Zwingmann, Degussa, 'Durch innere Oxydation dispersionsgehärteter Werkstoff', *German Appl.* 1,783,074; 1971

10 A. S. Darling, Johnson Matthey Co Ltd, 'Method of Making a Dispersion Strengthened Metal', *US Appl.* 3,696,502; 1972

11 S. Gärtner, D. Adam and W. Molle, *Neue Hütte*, 1979, **24**, (3), 103

12 B. Fischer, A. Behrends, D. Freund, D. F. Lupton and J. Merker, *Platinum Metals Rev.*, 1999, **43**, (1), 18

13 B. Fischer, K.-H. Goy, W. Kock, D. F. Lupton, H. Manhardt, J. Merker, F. Schölz and B. Zurowski, W. C. Heraeus GmbH & Co KG, 'Dispersion Strengthened Platinum Alloy and a Method for its Production', *European Patent* 0,870,844; 1998

14 S. Vorberg, B. Fischer, D. Lupton, M. Wenderoth, U. Glatzel and R. Völkl, 'Overview of the High-Temperature Mechanical Properties of Pt-Alloys', in "Second International Platinum Conference 'Platinum Surges Ahead'", Sun City, South Africa, 8th–12th October, 2006, Symposium Series S45, The Southern African Institute of Mining and Metallurgy, Johannesburg, South Africa, 2006

15 R. Bürgel, "Handbuch Hochtemperatur-Werkstofftechnik", Vieweg, Germany, 2001

16 J. Rösler and E. Arzt, *Acta Metall. Mater.*, 1990, **38**, (4), 671

17 B. Reppich, *Acta Mater.*, 1998, **46**, (1), 61

18 D. Häussler, M. Bartsch, U. Messerschmidt and B. Reppich, *Acta Mater.*, 2001, **49**, (18), 3647

19 A. Wasilkowska, M. Bartsch, U. Messerschmidt, R. Herzog and A. Czyrska-Filemonowicz, *J. Mater. Process. Technol.*, 2003, **133**, (1–2), 218

20 R. Behr, J. Mayer and E. Arzt, *Intermetallics*, 1999, **7**, (3–4), 423

21 Current and historical rhodium prices can be checked on Platinum Today at: http://www.platinum.matthey.com/pgm-prices/price-charts/ (Accessed on 24th August 2011)

22 R. Völkl, D. Freund and B. Fischer, *J. Test. Eval.*, 2003, **31**, (1), 35

23 R. Völkl and B. Fischer, *Exp. Mech.*, 2004, **44**, (2), 121

24 R. Völkl, B. Fischer, M. Beschliesser and U. Glatzel, *Mater. Sci. Eng.: A*, 2008, **483–484**, 587

25 P. J. Thomas and P. A. Midgley, *Ultramicroscopy*, 2001, **88**, (3), 179

26 R. F. Egerton, *J. Electron Microsc.*, 1999, **48**, (6), 711

27 D. Shindo and T. Oikawa, "Analytical Electron Microscopy for Materials Science", Springer, Berlin, Germany, 2002

28 A. Undisz, U. Zeigmeister, M. Rettenmayr and M. Oechsle, *J. Alloys Compd.*, 2007, **438**, (1–2), 178

29 S. Vorberg, R. Völkl, B. Fischer, D. Lupton and U. Glatzel, 'Microstructural Evolution during Creep of Oxide Dispersion Hardened Platinum Materials', Proceedings of the 28th International Precious Metals Conference, International Precious Metals Institute, Phoenix, Arizona, USA, 2004, pp. 48–68

30 K. C. Thompson-Russell and J. Edington, "Practical Electron Microscopy in Materials Science", Philips Technical Library, Palgrave Macmillan, Eindhoven, The Netherlands, 1976

31 R. Sandström, *Phys. Status Solidi A*, 1973, **18**, (2), 639

32 D. J. H. Cockayne, I. L. F. Ray and M. J. Whelan, *Philos. Mag.*, 1969, **20**, (168), 1265

33 J. H. Schröder and E. Arzt, *Scr. Metall.*, 1985, **19**, (9), 1129

34 J. Rösler and E. Arzt, *Acta Metall.*, 1988, **36**, (4), 1043

35 E. Arzt and J. Rösler, *Acta Metall.*, 1988, **36**, (4), 1053

36 M. Bartsch, A. Wasilkowska, A. Czyrska-Filemonowicz and U. Messerschmidt, *Mater. Sci. Eng.: A*, 1999, **272**, (1), 152

37 V. C. Nardone and J. K. Tien, *Scr. Metall.*, 1983, **17**, (4), 467

38 D. F. Lupton, J. Merker, B. Fischer and R. Völkl, 'Ductile High-Strength Platinum Materials for Glass Making', Proceedings of the 6th International Conference Advances in Fusion & Processing of Glass, Ulm, Germany, 29th–31st May, 2000

The Authors

Dipl.-Ing. Katharina Teichmann was a PhD student at the Department of Materials Science and Engineering at the Norwegian University of Science and Technology (NTNU). Her main work was transmission electron microscopy on aluminium alloys.

Dipl.-Ing. Christian Liebscher is a PhD student at the Chair of Metals and Alloys at the University of Bayreuth, Germany. His main interests include transmission electron microscopy, modelling and simulation in materials science and new high temperature materials.

Dr Rainer Völkl is academic councillor and senior researcher at the Chair of Metals and Alloys at the University of Bayreuth. His main fields of research include alloys of the platinum group metals as well as nickel-base alloys, testing of mechanical properties at high temperatures and electron microscopy.

Dr Stefan Vorberg is development project manager in the Technology Centre of the Engineered Materials Division of W. C. Heraeus GmbH, Germany. A main focus is the development of the oxide dispersion hardened platinum alloys (DPH materials) manufactured by Heraeus. Major interests are the applications of the materials and an understanding of the basic strengthening mechanisms.

Professor Dr Uwe Glatzel is head of the Chair of Metals and Alloys at the University of Bayreuth. His work had a big impact on the development of modern high temperature alloys, mainly nickel-base superalloys. He advises several research groups including platinum-based superalloys and alloys for high temperature applications, laser metallurgy, material analysis and artificial knee joints.

